Romanian Reports in Physics, Vol. 63, No. 3, P. 741–752, 2011

CONDENSED MATTER

OPTICALLY INDUCED BIREFRINGENCE OF A *p*-AMINOAZOBENZENE-EPOXY RESIN DERIVATIVE

T. BEICA[1], I. ZGURA[1], L. FRUNZA[1], P. GANEA[1], S. FRUNZA[1], L. DUMITRACHE[2], V. RADITOIU[2], and L. WAGNER[2]

[1]National Institute of Materials Physics, POBox MG 07, 077125 Magurele, Romania
E-mail: lfrunza@infim.ro
[2]National Institute for Research & Development in Chemistry and Petrochemistry, 060021 Bucharest, Romania

Received December 13, 2010

Abstract. A derivative of *p*-aminoazobenzene-epoxy resin was studied. Visually examination between crossed polarizers does not show birefringence but it can be optically induced. Changing the polarization direction of the irradiating light leads to the changing of the privileged direction of the induced birefringence. The birefringence value was evaluated and compared with liquid crystals as anisotropic compounds.

Key words: photoinduced birefringence, polarizing optical microscopy, differential scanning calorimetry, *p*-aminoazobenzene, coupled epoxy resin.

1. INTRODUCTION

It has been already demonstrated [1] that azo (-N=N-) groups bound to a polymer undergo photochemical *trans-cis-trans* isomerization and thermal *cis-trans* isomerization in the solid state. Then the investigation of azo compounds increased because of their potential applications ranging from optical components and lithography to sensors and smart materials. In fact, when linearly polarized light irradiates a film of azobenzene polymers, the azobenzene groups tend to align perpendicular to the polarization direction [2]. This is a photoisomerization phenomenon that can be used in interesting applications [3].

On the other hand, epoxy liquid-crystalline monomers with azo groups in the central mesogenic core, cross-linked with amines were also reported [4, 5].

The paper presents the properties of a recently synthesized epoxy material containing azobenzene units in the side chain. These proprieties were examined using polarizing optical microscopy, differential scanning calorimetry (DSC), spectroscopic methods. The focus of the study is to investigate possibilities of using irradiation to promote or control molecular orientation in this type of materials. Photoinduced birefringence was thus put in evidence and its kinetics

followed up, orienting the chromophore by irradiation is indeed found the cause which induces birefringence.

2. EXPERIMENTAL METHODS

2.1. MATERIALS

p-aminoazobenzene (m.p.=127°C, b.p.=366°C; min. 99%, provided by Merck) was crosslinked to Ropoxid 501 epoxy resin (having 0.53 equivalent epoxy/100g resin, M=377.36, supplied by Policolor): the curing recipe under microwaves was already described in detail [6]. In fact, the epoxy resin–amine mixture (with molar ratio resin/amine of 2.5) was prepared at room temperature by adding the curing agent while continuously stirring and then heating at a temperature less than the curing temperature until a homogeneous solution was obtained. The resulted compound has a low molecular weight (n~0.13) and its formula is given in Fig. 1. This compound still contains epoxy residues closing the main chain on both sides.

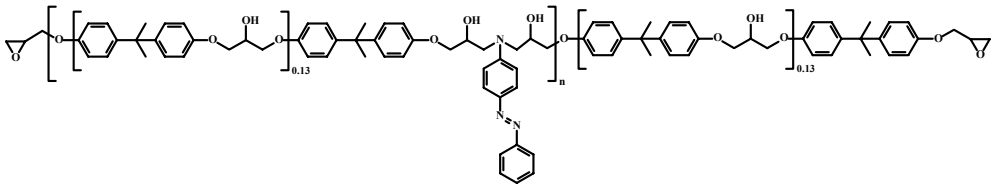

Fig. 1 – Chemical structure of the studied derivative.

Small amount of the material, which is solid at room temperature, has been melted by rapid heating to a temperature of 70°C, between two microscope slides (soda-lime type glass available from Cole Parmer), resulting layers with undetermined thickness. Pairs of the glass plates were held together in cells, using binder bulldog clips at two opposite ends. The cells were further used for optical investigations.

In some cases, a film was deposited onto a glass plate from a solution in easy evaporable solvent and was used as such especially for optical spectroscopy investigations.

2.2. METHODS OF INVESTIGATIONS

To characterize the obtained material, Fourier transform infrared spectroscopy (FTIR), optical spectroscopy, differential scanning calorimetry (DSC), termogravimetry-differential thermal analysis (TG-DTA) were applied. Thus,

vibrational spectra with a resolution of 4 cm^{-1} were recorded between 4000 and 400 cm^{-1} with a Jasco FTIR 6500 spectrometer and an ATR Specac Golden Gate attachment (30 scans were acquired). *UV-vis spectra* of solutions were measured in quartz cuvette with a Jasco V-570 spectrometer. The spectra of the films deposited onto glass plates were collected in transmission mode using a Perkin-Elmer Lambda 18 spectrometer. All the spectra were decomposed into (Gaussian) components using commercial programs as shown *e.g.* in ref. [7].

TG-DTA measurements were carried out using a Perkin Elmer Diamond apparatus under dry synthetic air at a heating rate of 10 degree/min. The data were processed as described elsewhere [8].

Phase transition behavior was studied with an apparatus DSC 204 F1 (Netzsch) at a scanning rate of 5 degree/min under protective atmosphere. Two to four runs of heating–cooling cycles were performed for each measurement. Calibrations in temperature and energy were carried out using standard values of indium and zinc.

The *presence and identification of the possible mesophases* in the prepared material was performed under crossed polarizers by direct visualization or in transmission mode with a polarized light microscope (Amplival Pol-u) equipped with a digital camera (Panasonic DMC-FZ8) and a heating stage (Instec) mounted onto the microscope stage. Consistent settings of both the microscope light source and the digital camera allowed for the direct comparison of images taken for different parts of the sample.

Optically induced birefringence and its dynamics (namely the rise, change and decay) was observed using a home made experimental set-up. Thus, the irradiation has been performed either with unfocused light coming from a incandescence bulb, the sample being protected from heating by adjusting its distance to the light source, or with polarized light from a laser. The set-up is sketched in the Fig. 2.

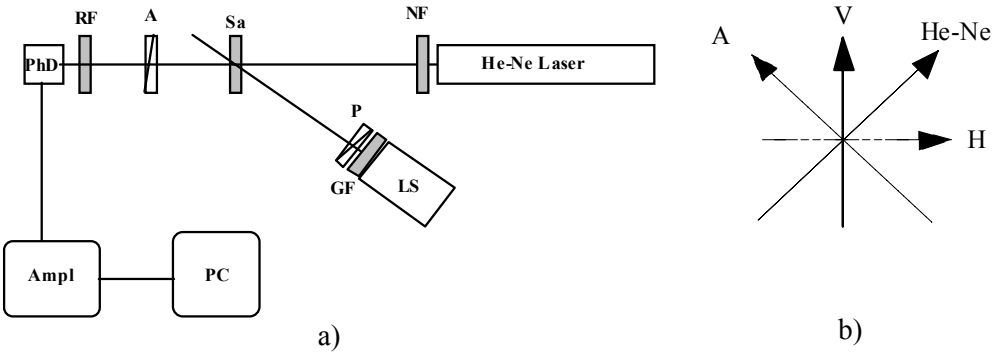

Fig. 2 – a) Sketch of the experimental setup: *NF* – neutral filter, *Sa* – sample, *A* – analyzer, *RF* – red filter, *PhD* – photodiode, *Ampl* – amplifier, *PC* – computer, *LS* – incandescent light source, *GF* – green filter, *P* – polarizer. b) Detail on the direction of the light polarization.

A He-Ne laser ($\lambda = 632.8$ nm, 5 mW) provides the measuring beam. It was polarized at 45° against the vertical axis in the figure, while the analyzer *A* is crossed to this direction. Photodiode *PhD* receives the light. The signal is amplified and then recorded (through an Axiom AX5411 card and a corresponding acquisition program) in the *PC* computer. A neutral filter *NF* attenuates the beam so that the diode response remains in the linear regime. At the same time a red filter *RF* (RG1, Schott Jena) is placed in front of the photodiode *PhD*; it let unmodified the laser beam but attenuates the green excitation light (as resulted from *LS* and *GF*) which would be a stray light for the detector.

The sample *Sa* is irradiated with exciting light at an incidence of 20° from a collimated source (*LS*) fitted with a green filter *GF* (VG6, Schott Jena). In choosing this filter we considered the following: a) to provide sufficient light (produced by an incandescent bulb) in the absorption band of the sample so that to optically induce the birefringence; b) to do not transmit much light through the filter *RF* which would increase the background at the detector.

The green excitation beam can be polarized by the polarizer *P* in two directions: in the incidence plane (polarization *H*) or perpendicular onto this (polarization *V*). Both directions are at 45° toward the laser polarization (Fig. 2b).

3. RESULTS AND DISCUSSION

Firstly the features of the studied derivative are presented. Then obtaining the optically induced birefringence is shown.

3.1. FEATURES OF THE *P*-AMINOAZOBENZENE-EPOXY RESIN DERIVATIVE

In the beginning the thermal stability of the material was checked by *TG-DTA measurements*. Fig. 3 represents the corresponding TG plot and indicates a thermal stability up to ca. 300°C followed by two losses in the weight, one smaller at 312°C and another one, around 400°C, very big. No processes related to melting of the epoxy part can be seen, but some thermal processes at the beginning of the heating might be related to the amine.

The temperature of possible phase transitions was pursued by DSC (see Fig. 4) in the limit of thermal stability; however, no clear phase transition peaks could be detected during either the heating or the cooling. The large endothermic process during the heating might be due to a post−curing process and/or to a glass transition which prevent phase transition peaks from being detected as in other similar cases [4, 5, 9]. Another reason might be the low content in azobenzene unit. For comparison, we have the phase transitions of a homopolymer based on

azobenzene [9] found at 74, 92 and 134°C by heating from the glass state to smectic, nematic and arriving at the isotropic state.

FTIR spectrum (Fig. 5) in the mid infrared region was obtained for the derivative as solution in chloroform. Epoxy band [5] at 914 cm^{-1} is still present in the spectrum supporting the sketched formula (Fig. 1). The identification of vibrational modes around 1 300–1 800 cm^{-1} is a very difficult task since the mixing of several bands is possible in this region. The N=N stretching appears at ca. 1 410 cm^{-1} and seems to be coupled [10] with the phenyl mode 19b (Wilson notation) at ca. 1 460 cm^{-1}. In fact, the phenyl ring modes manifest as (very) strong bands in IR spectra. A shift downward of the N=N stretching could be attributed to the presence of electron donating groups in *para* position [11]. The other aromatic ring stretching modes [12] are also visible in the spectrum. At 1 225 cm^{-1} the stretching of the aromatic eter link gives a strong absorption [13].

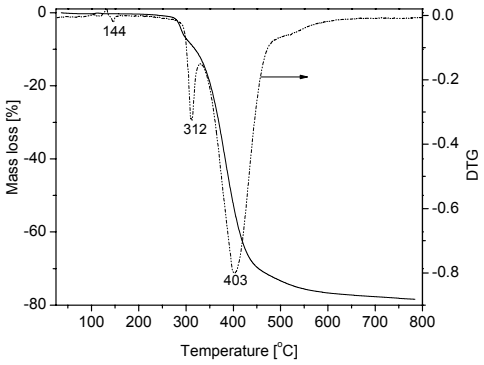

Fig. 3 – TG curve (continuous line) and its derivative DTG (dotted line) of the material.

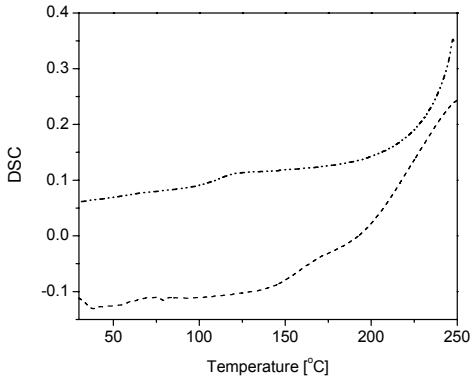

Fig. 4 – DSC curves obtained during the first heating (dashed line) and cooling (dot-dashed line).

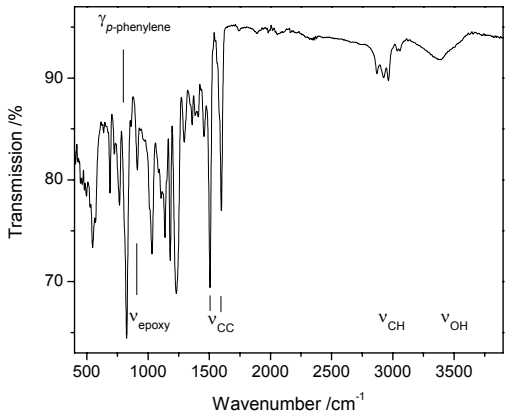

Fig. 5 – FTIR spectrum of the studied derivative and the assignment of main peaks.

A representative *UV-vis spectrum* of the studied derivative is shown in Fig. 6 together with its Gaussian components. There are three main absorptions at ca. 400, 497 and 623 nm and the queue of the glass cut toward UV region. The first peaks might be related to the azo groups under different environments.

It is worthy to note that the deposited material under the irradiation with the light (from an incandescence bulb) changes its spectrum (Fig. 6). Shift of the peak positions and intensity modifications are obvious by comparing the spectra in Fig. 6b. Thermal heating accompanying this irradiation leads to these spectrum changes as well. The assignment of these electronic bands starts from the well known azobenzene bands [14] and p-aminoazobenzene [11]: In this case, the $n \rightarrow \pi^*$ charge transfer transition near 440 nm may consist of two bands ascribed to the $n_a \rightarrow \pi^*$ and $n_s \rightarrow \pi^*$ transitions. A band at 320 nm is due to the $\pi \rightarrow \pi^*$ transition. Absorptions in the studied spectrum appear at 370, 403 and 438 nm.

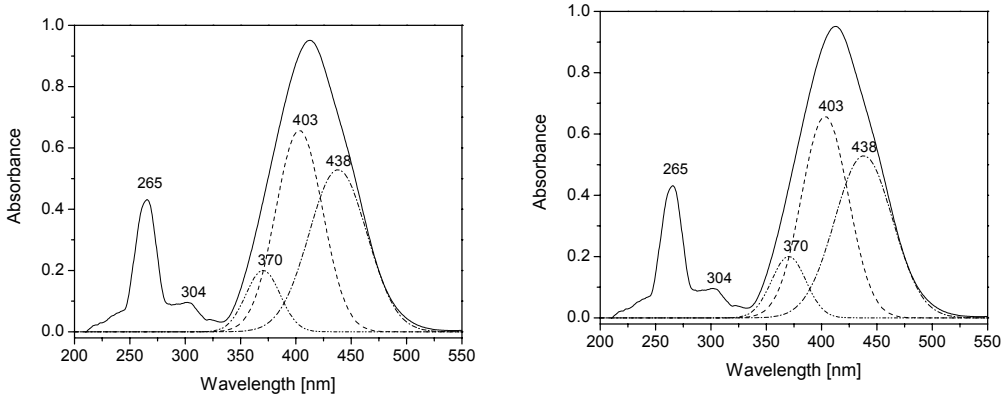

Fig. 6 – UV-Vis spectrum of the aminoazobenzene-epoxy resin derivative: a) in chloroform solution; b) comparison of the peak at ca 400 nm in the case of the sample solved in chloroform (1), deposited onto a glass plate (2) and deposited onto glass plate but after irradiation (3).

The molecular ratio of the forms *trans*:*cis* can be well estimated from the peak absorbance for $\pi \rightarrow \pi^*$ transition bands of *trans*-azobenzene units around 380 nm, assuming that the absorption of *cis*-azobenzene is negligible at this wavelength [11, 15, 16]. Since all azobenzene units exist as the stable *trans* form at the initial stage, the decrease of absorbance at 380 nm corresponds to the decrease of the *trans* form and the concomitant increase of the *cis* form. Comparison of the *cis/trans* composition among the three forms of stucied sample: solved in chloroform, deposited onto a glass plate and deposited onto glass plate but after 2h irradiation with incandescent light is obvious in Fig. 6b. The variation of the absorption maxima reflects the intermolecular interactions of the chromophores [17]. As expected, the absorption is larger in the solidified drop onto the glass than in the solution, but the deconvolution into Gaussians is rather similar (not shown).

Depending on the irradiation conditions, the photoisomerization reaches the plateau within 25 s [16], thus 2h might be considered as enough time to reach the *trans-cis* equilibrium in the case of our sample: this is easily seen by comparing the curve 2 with the curve 3 in Fig. 6b. The peak characteristic to the *trans* form decreased in intensity and that of the *cis* form increased by irradiation (the measurement was performed immediately after irradiation).

On the other hand, the presence of the mesophases in the material was additionally checked by *optical microscope observations* under crossed/parallel polarizers in transmission mode. The results are shown in Fig. 7.

One can observe the amorphous solid in Fig. 7a, which becomes dark under crossed polarizers (not shown), then the melt with some impurities went toward the edges in Fig. 7b and further (Fig. 7c), the solid obtained by cooling is again amorphous. No anisotropy was put there in evidence.

a) b) c)

Fig. 7 – Optical images (between parallel polarizers) of a cell filled with the studied derivative at temperatures as follows: a) 24.8ºC, during the heating; b) 90ºC, during the heating; c) 37ºC, during the cooling.

3.2. OPTICALLY INDUCED BIREFRINGENCE

The material studied did not show any birefringence when examined visually in low scattered light between crossed polarizers, meaning that we are dealing with an amorphous solid optically isotropic. However, if the sample area illuminated in polarized light was intense enough then this area shows a small but noticeable *birefringence induced under the polarized light of the optical microscope* is visually observable. Thus, by illumination, a privileged direction was induced into the sample, strictly related to the polarization direction of the irradiation light.

The optical birefringence was put in evidence by the transmission maximum at the examination between crossed polarizers when the easy direction makes an angle of 45^{o} with that of the polarizers. If the preferred direction was parallel to the polarizer or the analyzer, the transmission was minimal (virtually null). After ending the irradiation, the birefringence induced diminished up to disappearing in tens of minutes.

If the orientation of the polarization is changed during the irradiation changes of the induced easy direction and/or of the values of induced birefringence can be observed, so that after a while the sample presents the easy direction corresponding to the new polarization of the irradiation beam, as follows looking at the images obtained using the polarizing microscope: Fig. 8 shows four such images which were extracted from a video record by the microscope in polarized light. The sample is formed by the evaporation of a drop of the acetone solution of the material; this solid deposit has an identifiable topography. The images were recorded under crossed polarizers, the polarizer being parallel to the vertical axis of photographs, and the analyzer parallel to the horizontal axis. As a polarized beam of irradiation was used the light given by of the microscope source, passed through a polarizer and then focused.

Initially the sample did not present any intrinsic birefringence. Irradiation for about 5 minutes with the light provided by the microscope seems to do not change the former situation as shown in Fig. 8a; the dark appearance of the image can correspond both to the a birefringence lack and to the presence of one with a preferred direction parallel to one of crossed polarizers of the microscope. Rotating the sample by 45° (Fig. 8b) shows that the sample is clearly birefringent ($\Delta n \neq 0$) (the texture of the sample can be easily seen) and that this birefringence was induced by polarization of the incident light. Fig. 8c was recorded in the same polarized lighting conditions and sample orientation as the Fig. 8b. There is a net decrease in the image brightness image. This can be explained both by decreasing the birefringence (Δn) but also by re-orienting the privileged direction which can be induced by the new lighting conditions. Fig. 8d is obtained after sample return to the orientation taken in Fig. 7a but after irradiation Fig. 8b, Fig. 8d for about 50 s. The difference between Fig. 8a and 8d is obvious. This difference lies in their history, its origin being the orientation of the sample against the polarization direction of the incident beam and its cause being the sample interaction with the polarized light.

Measurements on the dynamics of the appearance, the modification and the decay of the optical birefringence induced in azo group containing sample lead to satisfactory results. However, such measurements have a big flaw: the (polarization) light with which the induced birefringence is detected is the same as the (polarized) light which induces the birefringence. That is why we performed other type of experiments as well. The green light irradiation at variance of the UV light irradiation at 350 nm < λ < 400 nm [18] was were selected with appropriate filters (see the Experimental part).

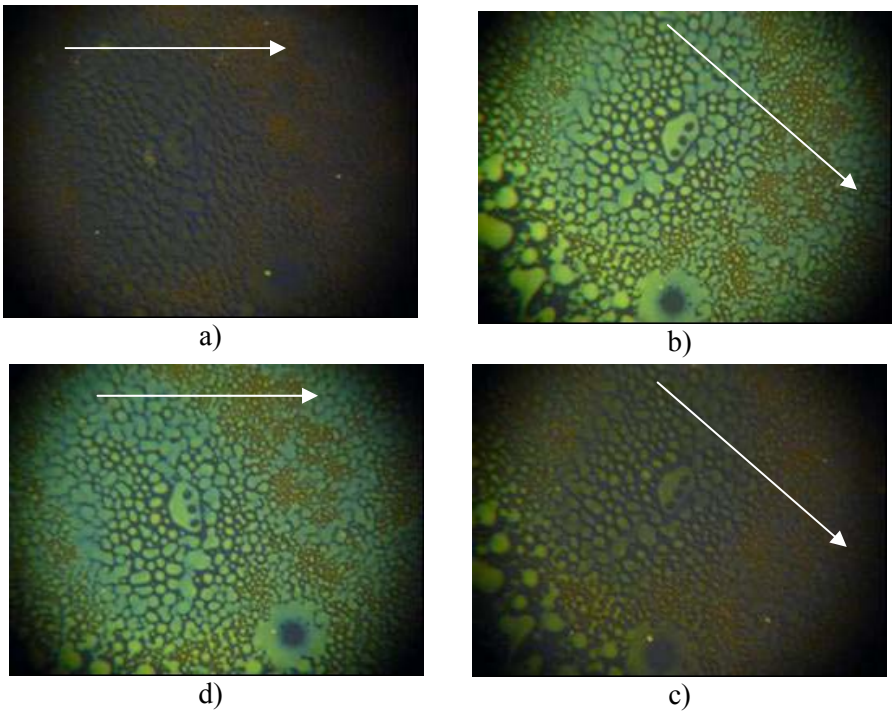

Fig. 8 – Images obtained using the polarizing microscope under the following conditions: a) after 5 min irradiation; b) rotating the sample from a) with 45º; c) the sample b) after "resting" 45 s without irradiation; d) rotating the sample c) to have the orientation as in a). The arrows indicate the sample orientation.

Typical time variation of the rise, change and decay for *birefringence induced under polarized light in the experimental set-up* is given in Fig. 9 when visual observation was performed in low diffuse light by rotating the sample between crossed polarizers.

Initially the sample did not present any significant birefringence. Sample irradiation with vertically polarized light induces a birefringence (zone *I*) related to the *V* orientation of the polarization of the irradiation beam. Changing its *V*-to-*H* or *H*-to-*V* polarization (the zones *R*1 and respectively *R*2) leads initially to a decrease in sample birefringence then followed by its growth. This may be related to the attenuation of preferred direction induced by the previous polarization and by the establishment of a new preferred direction imposed by the new beam polarization.

The last part of the record (the *S* zone) is the thermal decay of induced birefringence in the absence of polarized light beam; a characteristic exponential decay time of induced birefringence can be then estimated at $\tau_S \sim 250\,\mathrm{s}$. Also from the evolution of the record (zone *I*) one can estimate a characteristic time $\tau_I \sim 475\,\mathrm{s}$.

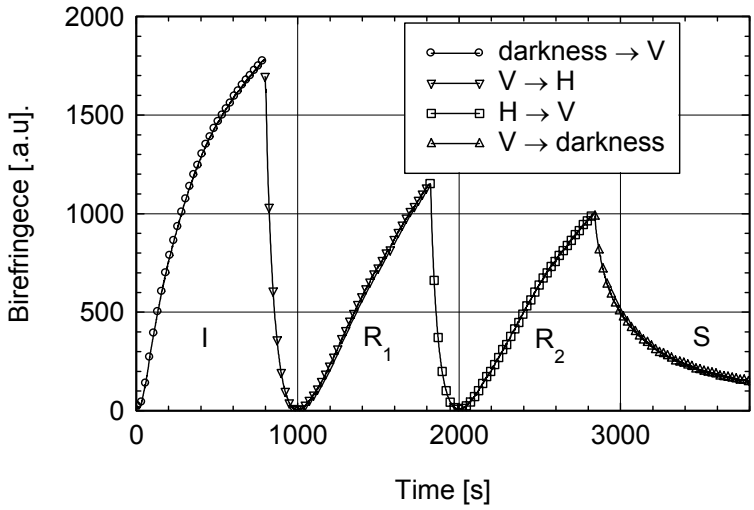

Fig. 9 – Time variation of the rise, change and decay for induced birefringence. The conditions are given in the legend.

The existence of a parasitic signal around 300 a.u. behaving like a jump at the onset (t = 0) or at the stop of the sample lighting ($R2$-S) with polarized light is observed. This is due to the fact that the transmission of the two used filters have a common portion of the light so that some "green" light can get as stray light from the photodiode which sees in "red" region.

We tried to estimate the size of the birefringence induced by the polarized light. A first estimate of the maximum transmission signal seen in Fig. 8 leads to a value $T \sim 0.07$. Considering that the law of variation of the sample transmission is of type:

$$T(\Delta n) = \sin^2\left(\frac{\pi d}{\lambda}\Delta n\right) \sim 0.07,$$

for $\lambda = 0.6328\ \mu\text{m}$ and for a sample thickness $d \sim 50\ \mu\text{m}$, one obtains a value of $\Delta n \sim 0.001$. This value is very low if it is compared to $\Delta n \sim 0.2$ which is specific for termotropic liquid crystals, such as classic 5CB, for which high values are explained both by the high degree of molecular ordering in liquid crystal state and by large differences in the molecular polarizability in the parallel or perpendicular direction along the molecular axis.

However, values of order of magnitude $\Delta n \sim 0.001$ were obtained for liotropic liquid crystals [19] as well. The small values of the Δn in the latter case are explained by the small difference in polarization properties along the long axis of the micelles and perpendicular to it although the order in this case is quite high, similar to that of termotropic liquid crystals.

Generally, the termotropic and liotropic liquid crystals have a high degree of ordering of their constituents (molecules or micelles, respectively), which provides the character of anisotropic intrinsic status to the state of liquid crystal.

In the case studied here we do not observe an intrinsic ordering of constituents (molecules or attached chromophores). The material do not have any intrinsic anisotropy in the solid/glass state or in the liquid state.

Low birefringence values obtained are explained by the nature of its inducing stimulus with an ordering character (here, polarized light). The value may depend on the intensity of the stimulus but the effect disappears after the disappearance of the stimulus in the absence of the events that would prevent the return of the partially ordered state (anisotropic) to a disordered state (isotropic).

Finally we determined the optical sign of birefringence induced by polarized light. Basically the induced birefringence can be determined, using a rotating compensator (Berek-type) and by rotating the sample with ±45º to the direction of polarization of the incident light, namely which of the refraction indices $n_{\parallel}$ or $n_{\perp}$ is higher: We defined the index of refraction $n_{\parallel}$ for light for "reading"; whose electric field is parallel to the sample "written"; with the electric field of light "writing"; that induced birefringence in the sample, namely the index of refraction $n_{\perp}$ for the case when the two directions are perpendicular. Using the previous notations we found $n_{\perp} > n_{\parallel}$.

4. CONCLUSIONS

The properties of a derivative obtained by coupling the *p*-aminoazobenzene to an epoxy resin were studied. The presence of the azo and epoxy groups was demonstrated spectroscopically. Transformation of the *trans* form into *cis* one was observed by irradiation with a white light. It was found as well that the derivative did not show any birefringence when it was examined (visually) in low scattered light between crossed polarizer, meaning that we are dealing with an amorphous solid (glass) optically isotropic.

The material has an optically induced birefringence, that was put in evidence by observing the behavior under crossed polarizers, after irradiation with polarized light. When the irradiation stops, this birefringence decreases in time and dissapears after some tens of minutes. Changing the polarization direction of the irradiating light leads to the changing of the privileged direction of the induced birefringence too. One can then suppose that this birefringence is linked to the azo chromophore groups and their *trans-cis-trans* mouvements.

The optical sign of birefringence induced by polarized light was then determined. The birefringence value was evaluated and compared with the values of liquid crystalline compounds.

Acknowledgements. The authors thank the financial support of National Authority for Scientific Research and of CNMP by the Project CLICOPOL/2007 of Research Development and Innovation National Program. The funding from COMAFI Project of CORE Program is acknowledged as well by some of the authors.

REFERENCES

1 C. S. Paik, H. Morawetz, Macromolecules, **5**, 172 (1972).
2 L. Corvazier, Y. Zhao, Macromolecules, **32**, 3195 (1999).
3 K.G Yager, C.J. Barrett, in *Polymeric Nanostructures and their Applications* (Ch. 8), H.C. Nalwa, (editor), Amer. Sci. Pub., Los Angeles, 2006.
4 P. Castell, M. Galià, and A. Serra, Macromol. Chem. Phys., **202**, 1649–1657 (2001).
5 M. Wlodarska, B. Mossety−Leszczak, G.W. Bak, H. Galina, and R. Ledzion, Opto-Electron. Rev., **17**, 105–111 (2009).
6 V. Rădiţoiu, L. Dumitrache, A. Rădiţoiu, S. Şerban, and L. Wagner, Mat. Plast., **47**, 130–134 (2010).
7 L. Frunza, S. Frunza, M. Poterasu, T. Beica, H. Kosslick, and D. Stoenescu, Spectrochim. Acta A, **72**, 248–253 (2009).
8 S. Frunza, H. Kosslick, A. Schönhals, L. Frunza, I. Enache, and T. Beica, J. Non-cryst. Solids, **325**, 103–112 (2003).
9 L. Cui, Y. Zhao, A. Yavrian, and T. Gals, Macromolecules, **36**, 8246–8252 (2003).
10 Z. Mei, G. Baranovic, V. Smrecki, P. Novak, G. Keresztury, and S. Holly, J. Molec. Struct, **408–409**, 399–403 (1997).
11 G. Eazhilarasi, R. Nagalakshmi, and V. Krishnakumar, Spectrochim. Acta A, **71**, 502–507 (2008).
12 D.G. Hanken, R.R. Naujok, J. M. Gray, and R.M. Corn, Anal. Chem., **69**, 240–248 (1997).
13 Y.C. Lin, Xu Chen, H.J. Zhang, and Z.P. Wang, Mater. Lett., **60**, 2958–2963 (2006).
14 H. H. Jaffé**,** S.-J. Yeh**,** and R. W. Gardner**,** J. Molec. Spectrosc., **2**, 120–136 (1958).
15 D.L. Beveridge, H.H. Jaffe, J. Am. Chem. Soc., **88**, 1948 (1966).
16 A. Izumi, M. Teraguchi, R. Nomura and T. Masuda, Macromolecules, **33**, 5347 (2000).
17 C. Racles, A. Airinei, A. Ioanid, C. Grigoras, and M. Cazacu, Rev. Roum. Chim., **52**, 117–125 (2007).
18 T. Umeyama, K. Kawabata, N. Tezuka, Y. Matano, Y. Miyato, K. Matsushige, M. Tsujimoto, S. Isoda, M. Takano, and H. Imahori, Chem. Commun, **46**, 5969–5971 (2010).
19 T. Beica, R. Moldovan, M. Tintaru, I. Enache, and S. Frunza, Cryst. Res. Technol., **39**, 151–156 (2004).